

Seismic study of the chemical composition of the solar convection zone

Chia-Hsien Lin

Astronomy Department, Yale University, P.O. Box 802101, New Haven, CT 06520-8101, U.S.A.

H. M. Antia

Tata Institute of Fundamental Research, Homi Bhabha Road, Mumbai 400005, India

and

Sarbani Basu

Astronomy Department, Yale University, P.O. Box 802101, New Haven, CT 06520-8101, U.S.A.

ABSTRACT

Recent downward revision of solar heavy-element abundances using three-dimensional atmospheric model has introduced serious discrepancies between standard solar models and helioseismic inferences about solar structure. In this paper, we investigate the possibility of determining the heavy-element abundances using helioseismic inversion techniques with the hope of providing an independent estimate. We use the adiabatic index, $\Gamma_1 \equiv (\partial \ln P / \partial \ln \rho)_s$, as a probe to examine the effects of the total heavy-element abundance, as well as the effects due to the abundance of individual elements. Our inversion results show that the new, lower, abundance increases the discrepancy between the Sun and the solar models.

Subject headings: Sun: abundances — Sun: oscillations — Sun: interior

1. Introduction

Until recently, various analyses had shown that the current standard solar models are in good agreement with the real solar structure to the order of 10^{-3} (see, e.g., Bahcall, Pinsonneault, & Wasserburg 1995; Gough et al. 1996; Bahcall, Pinsonneault, & Basu 2001;

Christensen-Dalsgaard 2002; Couvidat, Turck-Chièze, & Kosovichev 2003; Boothroyd, & Sackmann 2003; Richard, Théado, & Vauclair 2004). These standard solar models are usually constructed with OPAL equation of state (Rogers, Swenson, & Iglesias 1996; Rogers, & Nayfonov 2002), the OPAL opacity (Iglesias, & Rogers 1996), and the heavy-element abundances from Grevesse & Sauval (1998) or Grevesse, & Noels (1993). Recently, by using a three-dimensional hydrodynamical model atmosphere and improved atomic and molecular data, Allende Prieto, Lambert, & Asplund (2002); Asplund et al. (2004); Asplund, Grevesse, & Sauval (2005) revised the photospheric abundances for the most abundant heavy elements. The new abundances are markedly lower than the earlier values of Grevesse, & Sauval (1998) or Grevesse, & Noels (1993), and result in a total metallicity, $Z = 0.0122$, which is about 30% lower than the GS98 value of $Z = 0.0169$. The standard solar models implemented with the revised abundances deviate significantly from the solar structure as determined by the helioseismic analysis. In particular, the convection zone is too shallow and the helium abundance in the convection zone too low, which lead to poor match of the sound-speed and density profiles in the Sun (e.g., Basu, & Antia 2004; Bahcall et al. 2005a; Guzik, Watson, & Cox 2005; Turck-Chièze et al 2004). These models also have a different core-structure than the Sun (Basu et al. 2007). The discrepancy has triggered a great deal of interest in re-examining solar models. Various groups have explored the possibility of adjusting the opacity, diffusion rate, and neon abundance of the models to see if the discrepancy caused by the low abundances might be resolved. However, the attempts have not been successful (e.g., Basu, & Antia 2004; Bahcall et al. 2005a; Guzik 2006; Turck-Chièze et al 2004; Antia, & Basu 2006; Basu et al. 2007). Even invoking a different composition in the radiative interior through accretion Castro, Vauclair, & Richard (2007) fail to remove the discrepancy.

An independent spectroscopic analysis by Ayres, Plymate, & Keller (2006), which uses a thermal profile different from the one in Asplund et al. (2004), suggests an oxygen abundance that is closer to the previous value (i.e., Grevesse & Sauval 1998; henceforth GS98) than the most recent value (Asplund, Grevesse & Sauval 2005; henceforth AGS05). On the other hand, using 3-dimensional models with free parameters, Socas-Navarro & Norton (2007) find an oxygen abundance which is slightly lower than Asplund et al. (2004). Thus there appears to be considerable uncertainty in spectroscopic determinations of abundances, and it would be interesting to attempt an independent determination of abundances using the seismic data. Antia, & Basu (2006) carried out a helioseismic analysis to determine the heavy-element abundance. Their results suggest that $Z = 0.0172 \pm 0.002$, which is in good agreement with the value of Grevesse, & Sauval (1998). In that study, the abundance was estimated by using a dimensionless sound-speed gradient $W(r) = (r^2/Gm)(dc^2/dr)$, which deviates from the ideal-gas value of $-2/3$ in the ionization zones of elements. The deviation can then be used to measure the heavy-element abundances. However, because the ionization zones

of different heavy elements overlap, it is difficult to estimate their abundances separately. Hence, this analysis was used to estimate only the total heavy-element abundance, Z .

In this paper, we conduct a systematic study of the effects of both the total abundance and the element mixture by using another dimensionless quantity, the adiabatic index $\Gamma_1 \equiv (\partial \ln P / \partial \ln \rho)_s$ (s being the entropy). Our aim is to first identify the signatures due to the variation of the element abundance and then use this knowledge to assess the abundance difference between the Sun and the models.

Since the normally used equations of state (EOS), such as OPAL (Rogers, & Nayfonov 2002) and MHD (Däppen, Anderson, & Mihalas 1987; Däppen et al. 1988; Hummer, & Mihalas 1988; Mihalas, Däppen, & Hummer 1988), do not allow the user to change the chemical element mixture, and are currently available only with a fixed mixture, they are not suitable for our investigation. Instead, following Antia, & Basu (2006), we use the Eggleton, Faulkner, & Flannery (1973) equation of state with Coulomb corrections (Guenther et al. 1992; Christensen-Dalsgaard & Däppen 1992). This equation of state (referred to as CEFF, the ‘Coulomb-corrected’ EFF) includes all ionization states of 20 elements. The ionization fractions are calculated using only the ground state partition function. With the CEFF EOS we can specify the relative heavy-element abundance that we want to use, and hence, study the influence of different heavy-element mixtures. Studies have also shown that it gives a reasonable description of the thermodynamic structure of the solar material.

The reason for choosing the adiabatic index Γ_1 to probe the chemical composition is that it is sensitive to both the total abundance and the element mixture. Although Γ_1 also depends on temperature and density, these dependence can be separated from compositional variations if the EOS is known. The disadvantage of using Γ_1 is that the errors in the EOS also affect Γ_1 . The effects of the EOS errors and the composition errors might be entangled and difficult to separate. To systematically study the relation among Γ_1 , EOS and the chemical composition, we constructed a number of test models with different abundances and EOS. The test models and solar data used in this study are described in § 2, the inversion method is explained in § 3, and the results from the theoretical study and from using solar data are presented in § 4. Finally, § 5 summarizes the results of this study.

2. Solar data and models

We use solar oscillation frequencies obtained from data collected by the Michelson Doppler Imager (MDI) on board SOHO during its first 360 days of observations – 1996 May 1 to 1997 April 25. We refer to this as the MDI360 set (Schou et al. 1998). We have

chosen this set, since among the available helioseismic data for intermediate degree modes, this set was analyzed from the longest time series. Other sets have been obtained from much shorter, 72 or 108 days, time series. Solar oscillation frequencies are known to change with activity, and a longer time series would involve observations from periods of increasing solar activity, which would change the frequencies. It is well-established that solar oscillations frequencies increase with solar activity. However, it is also known that the increase is such that it does not reflect a change in structure of the solar interior (Basu 2002). The MDI360 set was obtained from a time series when solar activity was low. This helps minimize solar-cycle related frequency shifts, while providing lower errors than the 72 day sets. From the estimated errors in our results it is clear that the errors are acceptable for our work. It may be possible to improve the results by individually inverting all 72 day sets available for the entire solar cycle and then averaging the results.

To study the effects of the chemical composition, we use a series of models constructed with different compositions. Specifically, we constructed several models that have the same relative mixture of heavy-element abundances (either GS98 or AGS05) but different Z/X , ranging from 0.0165 to 0.0245, to examine the effect of metallicity. We also made models that have the same Z/X but with the abundance of some chemical elements either increased or lowered. It should be noted that the opacity tables or EOS for a solar model are calculated with a specified mixture of heavy elements that does not change with depth. The value of Z on the other hand is determined by specified value of Z/X at the surface and varies with depth due to diffusion. To increase the relative abundance of one element with respect to the rest without changing Z/X , the abundances of other elements is reduced to account for this adjustment in the mixture. Another alternative is to increase the abundance of one element and increase Z/X appropriately to keep the abundance of other elements at standard values. In some cases (e.g., for Neon) we have tried both options and the results can be compared. These models are static models calculated by solving the equations of stellar structure at a fixed age. Inputs needed are the hydrogen and heavy element abundance profiles (though not the absolute abundances). We have used the hydrogen and heavy element composition profiles from a solar model of Brun et al. (2002). The model incorporates diffusion of helium and heavy elements and mixing in the tachocline region. The composition profiles are scaled to the required values of X and Z . The exact structure of the models is not crucial for our work since we are looking at the intrinsic Γ_1 difference that depends only on the EOS and heavy element abundances. This difference does not depend on the difference in structure between the Sun and the model, nor does it depend on the difference in the helium abundance. Consequently, we do not make any special effort to get models with correct sound speed profile or the convection zone depth or the helium abundances. Nevertheless, these quantities for all models used in this work are listed in Table 1. In this table r_b is the position

of the base of the convection zone. These models use the OPAL opacity table computed for the appropriate heavy element mixture and use low temperature opacities from Kurucz (1991). The purpose of these models is to examine the signatures in the adiabatic index of differences in the relative mixture of heavy elements. Since Γ_1 reflects the effects of both the equation of state and the chemical composition, we constructed two models implemented with the latest version of the OPAL equation of state. These models are referred to as 245OPAL and 165OPAL, and have $Z/X = 0.0245$ and 0.0165 respectively. Because they are constructed with the OPAL EOS, the heavy-element mixture contains only four elements (C, N, O, Ne). In order to examine the effects resulting from the difference between CEFF and OPAL EOS, we have constructed two CEFF models that use the same mixture and Z/X as the OPAL models. These models with OPAL mixtures use the standard OPAL opacity tables to ensure that the difference is only due to EOS and not due to opacities. The properties of all models used in this paper are summarized in Table 1.

The relative difference in Γ_1 can be determined by helioseismic inversion. Although the complete set of oscillation modes can be computed for these models, we only used the modes that are also present in the observed data for the inversions between models in order to get realistic results. For the purpose of assessing the effect of the errors in the observed frequencies, we added random errors that are consistent with those in the observed frequencies to the model frequencies. The observational data set used for our mode selection is the aforementioned MDI360 data set.

3. Inversion procedures

The frequencies of solar oscillation modes depend on the solar structure. The starting point of helioseismic inversions is the linearization of the oscillation equations around a known solar model (the so-called reference model) using the variational principle. The frequency differences can then be related to the relative variations in sound speed (c) and density (ρ) between either two models or between the Sun and the reference model. The relation between the differences in frequency and these two variables (i.e., c and ρ) can be written as (Dziembowski, Pamyatnykh, & Sienkiewicz 1990; Antia, & Basu 1994):

$$\frac{\delta\omega_i}{\omega_i} = \int_0^R K_{c^2,\rho}^i(r) \frac{\delta c^2}{c^2}(r) dr + \int_0^R K_{\rho,c^2}^i(r) \frac{\delta\rho}{\rho}(r) dr + \frac{F_{\text{surf}}(\omega_i)}{Q_i} + \epsilon_i, \quad (1)$$

where c is the adiabatic sound speed, K^i are the kernels, and ϵ_i is the observational error in $\delta\omega_i/\omega_i$. $F_{\text{surf}}(\omega_i)/Q_i$ represents the effect of uncertainties in the model close to the surface, and is usually called the “surface term”. Here, Q_i is a measure of the mode inertia.

The structure variables, c^2 and ρ , in Eq. 1 can be converted into any other pair of independent variables. Specifically, for our study, we convert the variables c^2 and ρ to Γ_1 and P by using the relation $c^2 = \Gamma_1 P / \rho$ and the equation of hydrostatic equilibrium, which links the pressure and density. While the variable differences in Eq. 1 are the differences calculated at the same fractional *depth*, we are interested in the difference of Γ_1 compared at the same P and ρ (or any pair of thermodynamic variables). It is because comparing Γ_1 at the same P and ρ removes the effects due to the discrepancies in the main macro-physical properties (e.g., the solar structure variables P and ρ), and, hence, such $\delta\Gamma_1/\Gamma_1$ reflects only the microphysical (i.e., EOS) and composition discrepancies. To calculate $\delta\Gamma_1/\Gamma_1$ that represents only the microphysical discrepancies, which we call the “intrinsic” Γ_1 difference, we followed the technique proposed by Basu, & Christensen-Dalsgaard (1997):

$$\frac{\delta\Gamma_1}{\Gamma_1} = \left(\frac{\partial \ln \Gamma_1}{\partial \ln P} \right)_{Y,\rho} \frac{\delta P}{P} + \left(\frac{\partial \ln \Gamma_1}{\partial \ln \rho} \right)_{Y,P} \frac{\delta \rho}{\rho} + \left(\frac{\partial \ln \Gamma_1}{\partial Y} \right)_{P,\rho} \delta Y + \frac{\delta\Gamma_{1,\text{int}}}{\Gamma_1}, \quad (2)$$

where Y is the Helium abundance by mass, and $\delta\Gamma_{1,\text{int}}/\Gamma_1$ is the relative difference caused by the microphysical discrepancies. Consequently, the linear relation between $\delta\omega/\omega$ and $\delta\Gamma_{1,\text{int}}/\Gamma_1$ becomes:

$$\frac{\delta\omega_i}{\omega_i} = \int_0^R K_{u,Y}^i(r) \frac{\delta u}{u}(r) dr + \int_0^R K_{Y,u}^i(r) \delta Y(r) dr + \int_0^R K_{\Gamma_1,\rho}^i(r) \frac{\delta\Gamma_{1,\text{int}}}{\Gamma_1}(r) dr + \frac{F_{\text{surf}}(\omega_i)}{Q_i} + \epsilon_i, \quad (3)$$

where $u \equiv P/\rho$ is the isothermal sound speed. The functions $K^i(r)$ are known functions of the reference model.

We use the method of Optimally Localized Averages (OLA) to determine $\delta\Gamma_{1,\text{int}}/\Gamma_1$ by ‘inverting’ Eq. 3. The OLA technique (Backus & Gilbert 1968) attempts to produce a linear combination of data such that the resulting resolution kernel or ‘averaging kernel’ is suitably localized while simultaneously controlling the error estimates. Rabello-Soares et al. (1999) discuss the formulation of OLA inversion to study solar structures and how one may go about determining the inversion parameters for this type of an inversion.

The $\delta\Gamma_{1,\text{int}}/\Gamma_1$ in the formulation above has two contributions, one from differences in the equation of state, and another from differences in Z :

$$\frac{\delta\Gamma_{1,\text{int}}}{\Gamma_1} = \frac{\delta\Gamma_{1,\text{EOS}}}{\Gamma_1} + \frac{\partial \ln \Gamma_1}{\partial Z} \delta Z. \quad (4)$$

In principle, it should be possible to separate out the two parts, however, in practice we find that the limited number of mode frequencies make it difficult to get a reliable separation of the two quantities by inversions. Hence we limit ourselves to $\delta\Gamma_{1,\text{int}}/\Gamma_1$ in this work rather than its two components.

4. Results

4.1. What the models tell us

The first part of our study involves pairs of models and allows us to investigate the individual as well as combined effects on $\Gamma_{1,\text{int}}$ caused by differences in Z/X , the relative abundances of different elements, and the EOS. This also allows us to test our inversion technique. In order to do so, we use the frequency differences between two known models to infer $\delta\Gamma_{1,\text{int}}/\Gamma_1$ between them and then compare it with the known value. In this way, we can systematically investigate features resulting from different factors (e.g., differences in EOS, metallicity, relative composition, etc.) and whether these features can be determined reliably through inversions. This exercise enables us to determine whether we can discern subtle features at any level of significance with the currently available data sets. The knowledge gained from these tests helps to interpret the features obtained by inverting the frequency differences between the Sun and a known model.

In Fig. 1 we compare the exact and inverted $\delta\Gamma_{1,\text{int}}/\Gamma_1$ between two models. The inversions were carried out using only those modes that are present in the MDI360 mode set. We used the errors on the observed frequencies to determine the uncertainties in the inversion results. We see that we are able to obtain the differences successfully by inverting the frequency differences between the models. The inversion results however, are most accurate between about 0.77 and $0.92R_\odot$ for the mode set used. The limited number of high- l modes prevents us from inverting closer to the surface. This is unfortunate, since, the largest differences in $\delta\Gamma_{1,\text{int}}/\Gamma_1$ caused by differences in Z/X , EOS, or relative abundances of heavy elements occurs in the region $r > 0.95R_\odot$. However, we should still be able to make some inferences. The region $r > 0.95R_\odot$ would, in any case, be difficult to use for this work since the variation in Γ_1 in this region are dominated by HeII ionization, which overwhelms the much smaller signal due to ionization of heavy elements. The reason we cannot invert deeper than $0.77R_\odot$ is that we need to suppress the very large signature of u differences before the signature of the $\delta\Gamma_{1,\text{int}}/\Gamma_1$ differences can be extracted. The difference $\delta u/u$ is an order of magnitude or more larger just below the base of the convection zone and some part of the signal leaks into the lower part of the convection zone, thus making it difficult to suppress $\delta u/u$ contribution reliably in this region. This problem is more severe if the convection zone depth in the two models differ significantly. This results in either large errors, or very poor resolution, or both. In the rest of the paper, we shall therefore, concentrate only on the results for $r > 0.77R_\odot$.

In Fig. 2(a) we show $\delta\Gamma_{1,\text{int}}/\Gamma_1$ for models that have the same EOS and relative abundances, but different values of Z/X . We find that the difference in Z/X causes an almost

featureless parallel shift in the deeper regions ($r < 0.92R_{\odot}$), while there are deep depressions and small humps closer to the surface. The figure also shows the results obtained by inverting the frequency differences between the models. Unfortunately, the lack of high- l p-modes means that we cannot probe the region that shows the largest differences caused by Z/X . We can only probe the smaller parallel shifts at $r < 0.92R_{\odot}$. We find that for small differences in Z/X , as in the case of the models GS245 and GS230, $\delta\Gamma_{1,\text{int}}/\Gamma_1$ between the models below $r \approx 0.92R_{\odot}$ is comparable to the estimated errors. In other words, the inversion cannot distinguish between two models if the difference in Z/X is less than $\approx 6\%$.

The EOS used to construct our solar models are not perfect and are known to have differences with respect to the actual EOS of the solar matter (see e.g., Basu & Christensen-Dalsgaard 1997; Basu et al. 1999). Hence, to interpret results obtained with solar data, we need to know what type of differences are seen in $\Gamma_{1,\text{int}}$ because of EOS differences alone. For this purpose, we looked at the difference in $\Gamma_{1,\text{int}}$ between models constructed with the OPAL EOS and CEFF EOS. To ensure that the revealed features are solely due to the differences in EOS, we use CEFF models OM245 and OM165, that have the same heavy-element mixture as that implemented in OPAL EOS tables. Fig. 2(b) shows that for the same difference in Z/X between a pair of models, the difference in $\Gamma_{1,\text{int}}$ does not depend too much on the EOS used to construct the pair. The difference between OPAL and CEFF model pairs is of the order of the inversion errors. Fig. 2(c) shows the difference in $\Gamma_{1,\text{int}}$ between different EOS for models with the same composition. We can see that although the difference between the two EOSs causes very large features near the surface ($r > 0.93R_{\odot}$), the two EOSs are almost indistinguishable below $r \approx 0.90R_{\odot}$. We can very easily invert the $\Gamma_{1,\text{int}}$ differences between the two models in the region that is permissible by our mode sets. The fact that the two EOSs are indistinguishable throughout most of the convection zone also means that any solar result obtained using these CEFF models will be close to those obtained using OPAL models as long as we do not study regions very close to the surface.

Fig. 3(a) shows what happens when the abundance of any one element is increased. As can be seen, the different elements leave a distinct pattern. The changes shown in the figure are large enough to be seen in the inverted results. It should be noted that while for the model shown the abundances were changed by a factor of two, the oxygen abundance in the AGS05 and GS98 tables differ only by a factor of about 1.5 and the carbon abundance differs by a factor of about 1.35. The curve for neon is of interest since Antia & Basu (2005) had suggested that increasing the neon abundance by a factor of about 4 may bring the solar models constructed with the AGS05 abundances to have the correct position of the convection-zone base. Bahcall et al. (2005b) suggested a change by factor of between 2.5–3.5 to bring the convection-zone base and the convection zone helium abundance back into agreement with solar values. Similar results have been obtained by Zatri et al. (2007)

using the scaled small frequency separation in low degree modes. We see that adding neon makes the $\delta\Gamma_{1,\text{int}}$ positive below $0.9R_{\odot}$ and negative between 0.9 and $0.95R_{\odot}$. The results shown in Fig. 3(a) are however, somewhat disappointing in that it suggests that we could wipe out detectable changes in $\Gamma_{1,\text{int}}$ by, e.g., increasing the abundance of oxygen and carbon simultaneously. We could also increase the signal by reducing one element and increasing another, in other words, there may be multiple chemical compositions (with same Z/X) that may produce almost indistinguishable Γ_1 in the convection zone. This indicates that the chemical composition of the solar convection zone may not be uniquely determined from $\Gamma_{1,\text{int}}$. The cancellation effects may be seen in the $\Gamma_{1,\text{int}}$ differences between AGS05 and GS98 models with the same Z/X (Fig.3b). Another reason that the AGS05 and GS98 models with the same Z/X have such similar $\Gamma_{1,\text{int}}$ is that the relative abundances of the important elements like C,N,O and Ne between the GS98 and AGS05 abundance tables is almost the same, since these elements are reduced by almost identical factors in the AGS05 tables relative to the GS98 values. In general, the EOS is determined by the number density of different ions and the relative abundance by number of heavy elements with respect to hydrogen is of order of 10^{-4} . Hence the typical differences in Γ_1 due to variations in Z are of this order as can be seen from Figs. 1,2. In the case of difference between GS98 and AGS05 mixtures with the same Z , the differences in relative abundances are much smaller and hence the effect is also very small.

4.2. Results with solar data

The inversion results of $\delta\Gamma_{1,\text{int}}/\Gamma_1$ between the Sun and various reference models are presented in the Figures 4, 5 and 6. The inversion results using the solar data MDI360 and various models are shown in Fig. 4. The first notable inference is that models with $Z/X = 0.0165$ are more discrepant with respect to the Sun than models with $Z/X = 0.0245$ or $Z/X = 0.023$. This is yet another result that shows that the Sun has a higher Z/X than that given by AGS05. The difference between the Sun and models with $Z/X = 0.0165$ appear to be the same regardless of whether the models were constructed with the GS98 or AGS05 relative heavy-element abundances. This is not surprising given the results in Fig.3(b) discussed earlier. Thus using our inversions we cannot say whether the GS98 or AGS05 relative heavy-element mixture is closer to that in the Sun. We can only say that the AGS05 model with $Z/X = 0.0165$ does not match the solar Γ_1 . For OPAL models too the agreement with the Sun is worsened for $Z/X = 0.0165$. It may be noted that in this case the OPAL models use a very different heavy-element mixture as compared to other models, which would also account for some of the differences.

Even though the $\delta\Gamma_{1,\text{int}}/\Gamma_1$ differences between the Sun and the models with $Z/X = 0.0245$ and $Z/X = 0.023$ are visibly different, the difference in the region $0.77R_\odot < r < 0.90R_\odot$ is comparable to the magnitude of the inversion errors. Despite the difference between CEFF and OPAL, Fig. 4 shows that the solar models implemented with either OPAL or CEFF equation of state favor the previous heavy-element abundance (i.e., $Z/X = 0.0245$ and 0.0230) over the latest, lower value, $Z/X = 0.0165$. Hence, based on the precision of current helioseismic data, models with either $Z/X = 0.0245$ or $Z/X = 0.0230$ are equally plausible.

We find that for the same value of $Z/X = 0.0245$, enhancing the carbon abundance of a model brings it in closer agreement with the Sun, as is shown in Fig. 5. As can also be seen, enhancing the oxygen abundance actually worsens the agreement, particularly when compared to a model with a normal GS98 relative heavy-element abundance. Given that one of the suggestions to improve models constructed with AGS05 abundances was to increase the neon abundance (Antia & Basu 2005; Bahcall et al. 2005b), we turn our attention to models with enhanced neon abundance. Antia & Basu (2005) had suggested a neon enhancement by a factor of about 4. Keeping all other elemental abundances at the AGS05 level, this would imply a Z/X of 0.0209. We first look at models with $Z/X = 0.0209$ with and without neon enhancement to disentangle the effects of neon enhancement from those of increased Z/X . The results are shown in Fig. 6(a). What we see is that enhancing neon actually worsens the agreement with the Sun in the deeper part of the convection zone, but makes the agreement better above about $0.90R_\odot$. However, the neon enhanced models are better than models with the unmodified AGS05 relative abundances and the AGS05 total metallicity of $Z/X = 0.0165$ as can be seen in Fig. 6(b). We can also see that the model with neon enhanced by a factor of two and C,N,O increased by an amount corresponding to their 1σ errors in the AGS05 tables (which was another suggestion of Antia & Basu 2005) also give a better agreement than the plain AGS05 model. However, neither of these models fare as well as the model with GS98 abundances and abundance ratios. Thus it appears that the improvement relative to AGS05 models is more due to the increased Z/X in the neon enhanced models, than due to the enhancement of neon. Thus while enhancing neon brings the position of the convection-zone base of the solar models in agreement with that of the Sun, the discrepancy in the adiabatic index remains to a large extent.

5. Summary

In this work we examine the difference in adiabatic index, Γ_1 between the Sun and different solar models. Our aim is to determine whether this can be used to determine the

heavy-element abundances in the convection zone. In order to examine the effect of heavy-element abundances on Γ_1 , we use the so-called ‘intrinsic’ Γ_1 differences, between the Sun and the models, i.e., differences in Γ_1 at the same pressure, density and helium abundance. What remains when these dependences are removed are Γ_1 differences caused by differences in the equation of state and by differences in the heavy-element abundances. For convenience we call these the $\Gamma_{1,\text{int}}$ differences. These differences do not depend on differences in structure or helium abundance. We first use a series of models to test the sensitivity of the inversions and also to determine separately what type of $\Gamma_{1,\text{int}}$ differences are caused by differences in the total metallicity, i.e. Z/X , differences in the equation of state and differences in the relative abundances of heavy elements. From the study of models we find that our inversion results are reliable in the region $0.77 \leq r \leq 0.92R_\odot$. In this regions Z/X differences cause an almost parallel shift of the $\delta\Gamma_{1,\text{int}}$ curve. EOS differences appear only for $r > 0.90R_\odot$. Enhancing the abundance of one element gives humps at different radii, however, if two or more elements are changed the features can largely cancel out in some cases. Because of these effects, it is not possible to distinguish between the relative heavy-element abundances of the GS98 and the AGS05 mixtures.

Using solar data we find that models constructed with $Z/X = 0.0165$, i.e., the total metallicity of AGS05, are not consistent with the Sun. The $\Gamma_{1,\text{int}}$ for these models are lower than that of the Sun in the region of the convection zone that we can study. Models with $Z/X = 0.023$, i.e., GS98 total metallicity fare much better and confirm the results of Antia & Basu (2006), who used the dimensionless sound speed gradient inside the convection zone. There are however, discrepancies between the $Z/X = 0.023$ models and the Sun close to the surface, which probably point to differences in EOS between our models and the Sun. These results thus add to the list of discrepancies between models with AGS05 metallicities and the seismic data. As mentioned earlier, the discrepancy between the position of the convection-zone base was the first to be noted. Since then we know that the models are also deficient in the core (Basu et al. 2007; Zaatari et al. 2007), and also in the dimensionless gradient of the sound speed in the convection zone (Antia & Basu 2006). Now we can add the discrepancy in Γ_1 in the convection zone to that list. It may be noted that the discrepancy in the depth of the convection zone, the helium abundance in the convection zone or in the core structure are due to differences in opacity caused by reduction in Z . In principle, these can be resolved if the opacities are revised upwards by 10–20% (Basu & Antia 2004; Turck-Chièze et al. 2004; Bahcall et al. 2005a). However, the discrepancies in the dimensionless sound speed gradient or Γ_1 will not be affected by increasing the opacity. Thus it is clear that revision of opacity of solar material will not resolve all discrepancies. While the dimensionless sound speed gradient does depend weakly on the density profile or convection zone depth, the difference $\delta\Gamma_{1,\text{int}}$ studied in this work is obtained by correcting for

these differences and hence depends only on the EOS and heavy-element abundances. It may be argued that changing Z would also change X or Y , which could indirectly affect Γ_1 . This is not expected since in the region that we are studying, $r < 0.92R_\odot$, hydrogen and helium are fully ionized and will not contribute to departure of Γ_1 from $5/3$. The exact location of ionization zones of various elements depends on treatment of EOS and there could be some error in these due to uncertainties in EOS. However, since two independent EOS are giving similar results we expect that these errors are not too large. Judging by the nature of the $\Gamma_{1,\text{int}}$ differences between AGS05 models and the Sun, EOS errors are unlikely to explain the difference. From our results we can estimate the Z/X value in the Sun to be around 0.023.

Looking at the differences in intrinsic Γ_1 (Fig. 4) it appears that the discrepancy in the region $r > 0.85R_\odot$ is probably due to EOS. We may expect the EOS discrepancy to reduce in deeper layers as we move away from the HeII ionization zone. In view of this discrepancy it may be difficult to determine the value of Z/X , but a value close to 0.023 appears to be preferred over smaller values. It is possible to further decompose $\delta\Gamma_{1,\text{int}}$ in terms of EOS contribution and another contribution from Z or even Z_i the abundances of each heavy element. Because of the discrepancy in EOS and the fact that the ionization zones of different heavy elements overlap, it may be difficult to determine individual Z_i , but it may still be possible to determine total Z .

Since an increased neon abundance has been suggested (Antia & Basu 2005; Bahcall et al. 2005b) as a possible solution to resolve the discrepancy between solar models and seismic data, we examine the models with enhanced neon abundance. We find that the models with the abundance of neon enhanced with respect to the AGS05 values do better than the AGS05 models, but the improvement appears to be a result of an increase in Z/X rather than an increase in the neon abundance — increasing neon while keeping Z/X fixed makes the agreement between the Sun and models worse. Thus it appears that increasing neon abundance alone does not help in resolving the discrepancy. It is necessary to increase the abundances of other elements like oxygen too. Increasing Ne abundance over the GS98 abundances may lead to better agreement with seismic data. But it is difficult to make any definitive statement as it will also depend on the EOS. It may help if more sophisticated EOS tables are available for different element mixtures.

Our investigation is handicapped by the lack of high degree modes in the set. Differences in $\Gamma_{1,\text{int}}$ caused by errors in the equation of state or heavy-element abundances are largest above $0.95R_\odot$. High-precision frequencies of high degree modes are needed to investigate the effects of equation of state and abundances on the adiabatic index properly. However, the study indicates that the heavy-element abundance of the Sun is significantly higher than that suggested by Asplund et al. (2005) and close to that of Grevesse & Sauval (1998).

Acknowledgments

We would like to thank the Referee for comments that have led to improvements in the paper. We thank the OPAL group for the online opacity tables with different heavy-element mixtures and the updated EOS tables. This work utilizes data from the Solar Oscillations Investigation / Michelson Doppler Imager (SOI/MDI) on the Solar and Heliospheric Observatory (SOHO). SOHO is a project of international cooperation between ESA and NASA. MDI is supported by NASA grant NAG5-8878 to Stanford University. This work is partially supported by NSF grant ATM 0348837 to SB.

REFERENCES

- Allende Prieto, C., Lambert, D. L., & Asplund, M. 2002, *ApJ*, 573, L137
- Antia, H. M. and Basu, S. 1994, *A&AS*, 107, 421
- Antia, H. M. and Basu, S. 2005, *ApJ*, 620, L129
- Antia, H. M. and Basu, S. 2006, *ApJ*, 644, 1292
- Asplund, M., Grevesse, N., & Sauval, A. J. 2005, in *ASP Conf. Ser. 336: Cosmic Abundances as Records of Stellar Evolution and Nucleosynthesis*, ed. T. G. Barnes & F. N. Bash, 25 (AGS05)
- Asplund, M., Grevesse, N., Sauval, A. J., Allende Prieto, C., and Kiselman, D. 2004, *A&A*, 417, 751
- Ayres, T. R., Plymate, C., & Keller, C. U. 2006, *ApJS*, 165, 618
- Bahcall, J. N., Basu, S., Pinsonneault, M., & Serenelli, A. M. 2005a, *ApJ*, 618, 1049
- Bahcall, J. N., Basu, S., Serenelli, A. M. 2005b, *ApJ*, 631, 1281
- Bahcall, J. N., Pinsonneault, M. H., & Basu, S. 2001, *ApJ*, 555, 990
- Bahcall, J. N., Pinsonneault, M. H., & Wasserburg, G. J. 1995, *Rev. Mod. Phys.*, 67, 781
- Basu, S. 2002, in *From Solar Minimum to Maximum: Half a Solar Cycle with SOHO*, Ed. A. Wilson, ESA SP-508, Noordwijk, p. 7
- Basu, S. & Antia, H. M. 2004, *ApJ*, 606, L85

- Basu, S., Chaplin, W.J., Elsworth, Y., New, R., Serenelli, A.M., Verner, G.A. 2007, *ApJ*, 655, 660
- Basu, S. & Christensen-Dalsgaard, J. 1997, *A&A*, 322, L5
- Basu, S., Däppen, W., Nayfonov, A. 1999, *ApJ*, 518, 985
- Brun, A. S., Antia, H. M., Chitre, S. M. & Zahn, J.-P. 2002, *A&A*, 339, 239
- Boothroyd, A. I. & Sackmann, I.-J. 2003, *ApJ*, 583, 1004
- Castro, M., Vauclair, S., Richard, O. 2007, *A&A*, 463, 755
- Christensen-Dalsgaard, J. 2002, *Rev. Mod. Phys.*, 74, 1073
- Christensen-Dalsgaard, J., Däppen, W. 1992, *A&ARv*, 4, 267
- Couvidat, S., Turck-Chièze, S., & Kosovichev, A. G. 2003, *ApJ*, 599, 1434
- Däppen, W., Anderson, L., & Mihalas, D. 1988, *ApJ*, 319, 195
- Däppen, W., Mihalas, D., Hummer, D. G., & Mihalas, B. W. 1988, *ApJ*, 332, 261
- Delahaye, F. & Pinsonneault, M. H. 2006, *ApJ*, 649, 529
- Dziembowski, W. A., Pamyatnykh, A. A., & Sienkiewicz, R. 1990, *MNRAS*, 244, 542
- Eggleton, P. P., Faulkner, J., & Flannery, B. P. 1973, *A&A*, 23, 325
- Gough, D. O., Kosovichev, A. G., Toomre, J., et al. 1996, *Science*, 272, 1296
- Grevesse, N. & Noels, A. 1993, in *Proc: Origin and evolution of the elements*, eds. N. Prantzos, E. Vangioni-Flam, M. Casse, (Cambridge: Cambridge University Press), 14
- Grevesse, N. & Sauval, A. J. 1998 in *Solar Composition and Its Evolution - From Core to Corona*, ed. Fröhlich, C., Huber, M. C. E., Solanki, S. K., & von Steiger, R., 161 (GS98)
- Guenther, D. B., Demarque, P., Kim, Y.-C., & Pinsonneault, M. H. 1992, *ApJ*, 387, 372
- Guzik, J.A., 2006 in *Proc. SOHO 18/GONG 2006/HELAS I*, ESA-SP 624, ed., K. Fletherm M.J. Thompson, 17.1
- Guzik, J. A., Watson, L. S., & Cox, A. N. 2005, *ApJ*, 627, 1049
- Hummer, D. G. & Mihalas, D. 1988, *ApJ*, 331, 794

- Iglesias, C. A. & Rogers, F. J. 1996, *ApJ*, 464, 943
- Kurucz, R. L. 1991, in *Stellar Atmospheres: beyond classical models*, ed. L. Crivellari, I. Hubeny, and D. G. Hummer, NATO ASI series, Kluwer, Dordrecht, p. 441.
- Mihalas, D., Däppen, W., & Hummer, D. G. 1988, *ApJ*, 331, 815
- Rabello-Soares, M.C., Basu, S., Christensen-Dalsgaard, J., 1999, *MNRAS*, 309, 35
- Richard, O., Théado, S. & Vauclair, S. 2004, *Sol. Phys.* 220, 243
- Rogers, F. J. & Nayfonov, A. 2002, *ApJ*, 576, 1064
- Rogers, F. J., Swenson, F. J., & Iglesias, C. A. 1996, *ApJ*, 456, 902
- Socas-Navarro, H. & Norton, A. A. 2007, *astro-ph/0702162*
- Schou, J., Christensen-Dalsgaard, J., Howe, R., et al. 1998, in *Structure and Dynamics of the Interior of the Sun and Sun-like Stars SOHO 6/GONG 98 Workshop Abstract*, June 1-4, 1998, Boston, Massachusetts, ed. Korzennik, S., 845
- Turck-Chièze, S., Couvidat, S., Piau, L., Ferguson, J., Lambert, P., Ballot, J., García, R. A. & Nghiem, P. 2004, *Phys. Rev. Let.*, 93, 211102
- Zaatri, A., Provost, J., Berthomieu, G., Morel, P. & Corbard, T. 2007, *A&A* (in press) [arXiv:0704.2294](https://arxiv.org/abs/0704.2294)

Table 1: OPAL and CEFF Models

Model Name	Z/X	Y	r_b/R_\odot	Mixture	Enhancements
Models with OPAL EOS					
165OPAL	0.0165	0.2151	0.7252	OpalMix ¹	
245OPAL	0.0245	0.2496	0.7153	OpalMix ¹	
Models with CEFF EOS					
OM165	0.0165	0.2147	0.7284	OpalMix ¹	
OM245	0.0245	0.2494	0.7181	OpalMix ¹	
GS245	0.0245	0.2571	0.7203	GS98 ²	
GS230	0.0230	0.2514	0.7218	GS98 ²	
GS165	0.0165	0.2216	0.7303	GS98 ²	
AGS165	0.0165	0.2313	0.7319	AGS05 ³	
AGS209	0.0209	0.2530	0.7258	AGS05 ³	
A209Ne2	0.0209	0.2511	0.7220	AGS05* ⁴	2×Ne
A209Ne4	0.0209	0.24771	0.7171	AGS05* ⁴	4×Ne
A197Ne2CNO	0.0197	0.2394	0.7219	AGS05* ⁴	2×Ne; enhance C,N,O by 1 σ
GC2	0.0245	0.2418	0.7210	GS98* ⁵	2×C
GO2	0.0245	0.2291	0.7154	GS98* ⁵	2×O
GNe2	0.0245	0.2554	0.7156	GS98* ⁵	2×Ne
GO1.5C1.5	0.0245	0.2344	0.7176	GS98* ⁵	1.5×(C, O)

¹ OpalMix: mixture used in OPAL EOS

² GS98: mixture of Grevesse, & Sauval (1998)

³ AGS05: mixture of Asplund, Grevesse, & Sauval (2005)

⁴ AGS05*: AGS05 with enhancements of certain elements as noted under column ‘Enhancements’

⁵ GS98*: GS98 with enhancements of certain elements as noted under column ‘Enhancements’

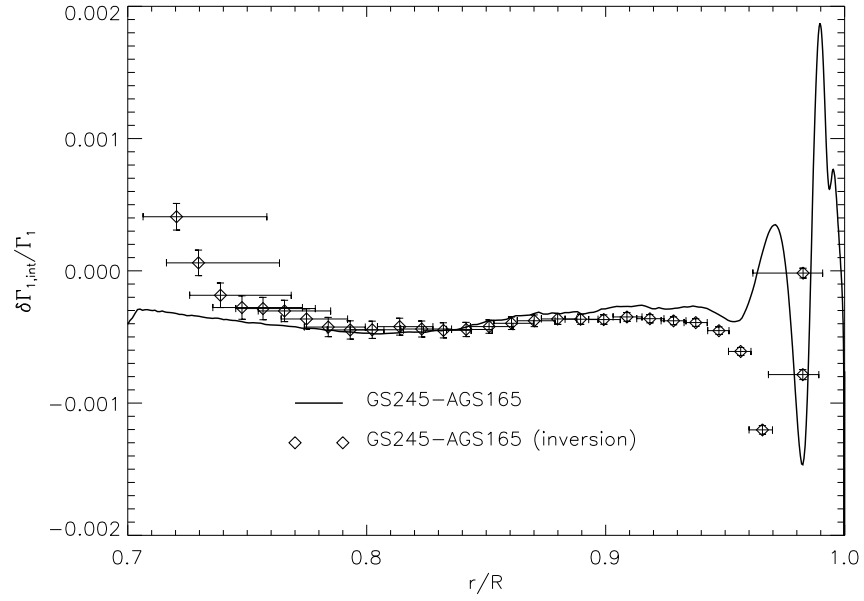


Fig. 1.— A comparison of the inverted and the exact $\Gamma_{1,\text{int}}$ differences between two models. The line is the exact results, the points with the error bars are the results obtained by inverting the frequency differences between the two models using only the modes in the MDI360 set. The vertical error bars are a measure of the uncertainties caused by errors in the frequencies. The horizontal error bars are a measure of the resolution of the inversion.

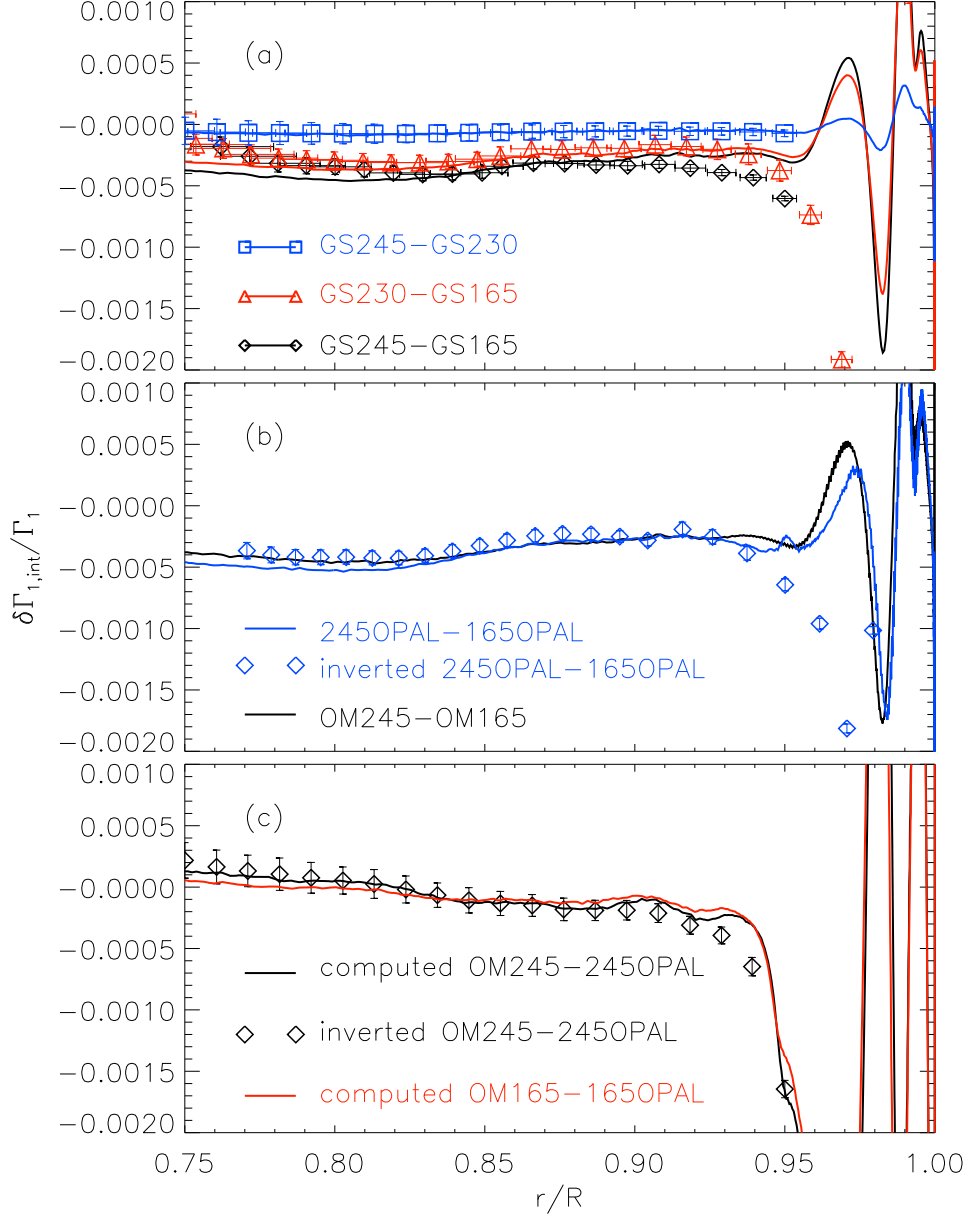


Fig. 2.— The $\Gamma_{1,\text{int}}$ differences between different pairs of models. Panel (a) illustrates the effect of changing Z/X . Panel (b) shows the response of models with different equations of state to changes in Z/X . Panel (c) shows what happens when the models have the same Z/X and relative heavy element abundances, but different equations of state. In all panels the lines are the exact results, and the points are the results obtained by inverting the frequency differences between the pairs of models.

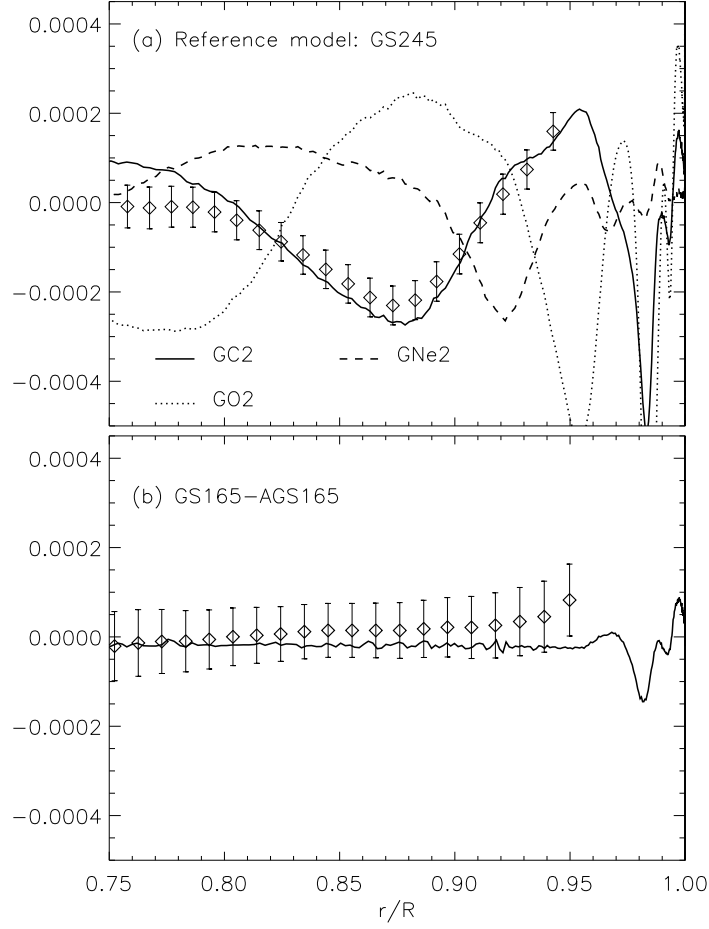


Fig. 3.— The effect of changes in the relative heavy-element abundances keeping Z/X the same. Panel (a) shows the effect when one of the elements is enhanced by a factor of 2. Panel (b) shows the $\Gamma_{1,\text{int}}$ differences between two models, both with $Z/X = 0.0165$, but one constructed with the GS98 relative heavy-element abundance and the other the AGS05 relative heavy-element abundance.

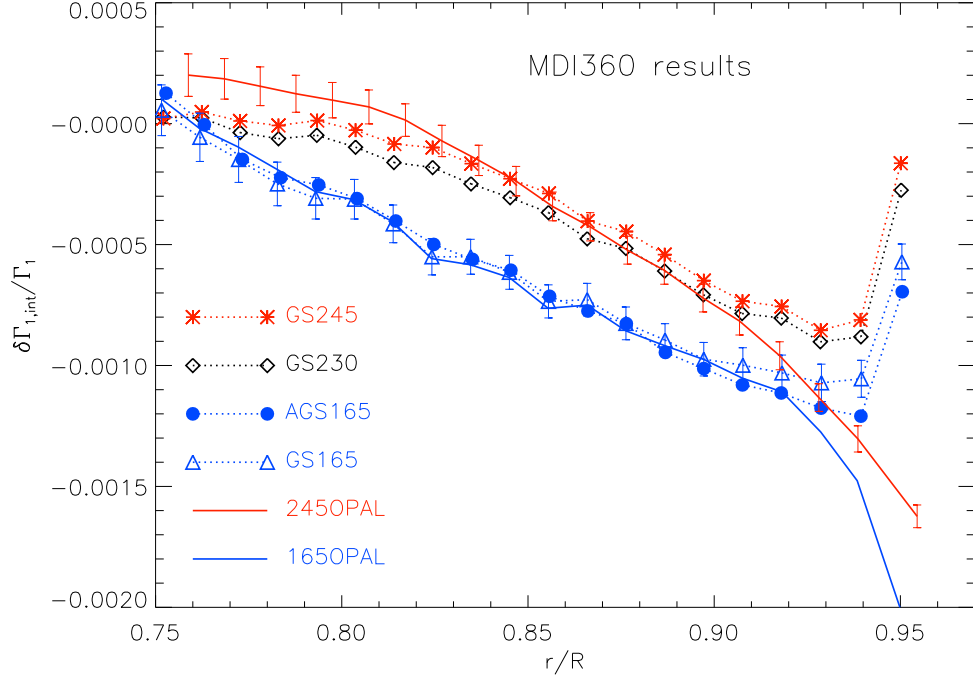


Fig. 4.— Differences in $\Gamma_{1,\text{int}}$ between the Sun and different models obtained by inverting the frequency differences between the Sun and the models. The models are described in Table 1.

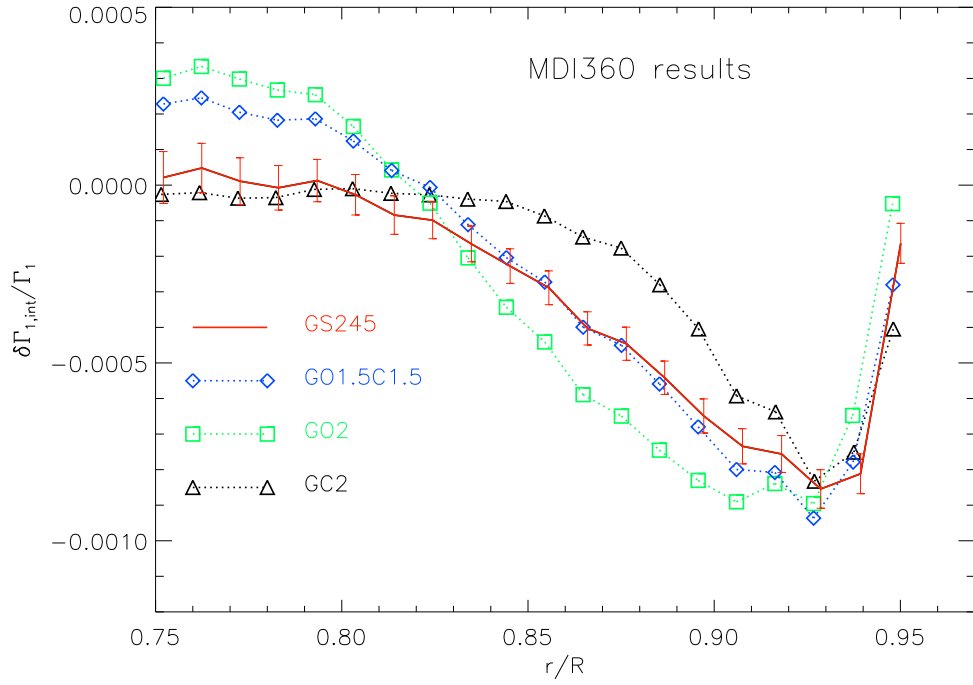


Fig. 5.— The $\Gamma_{1,\text{int}}$ differences between the Sun and models with the abundance of some elements changed. The value of Z/X is the same for all models.

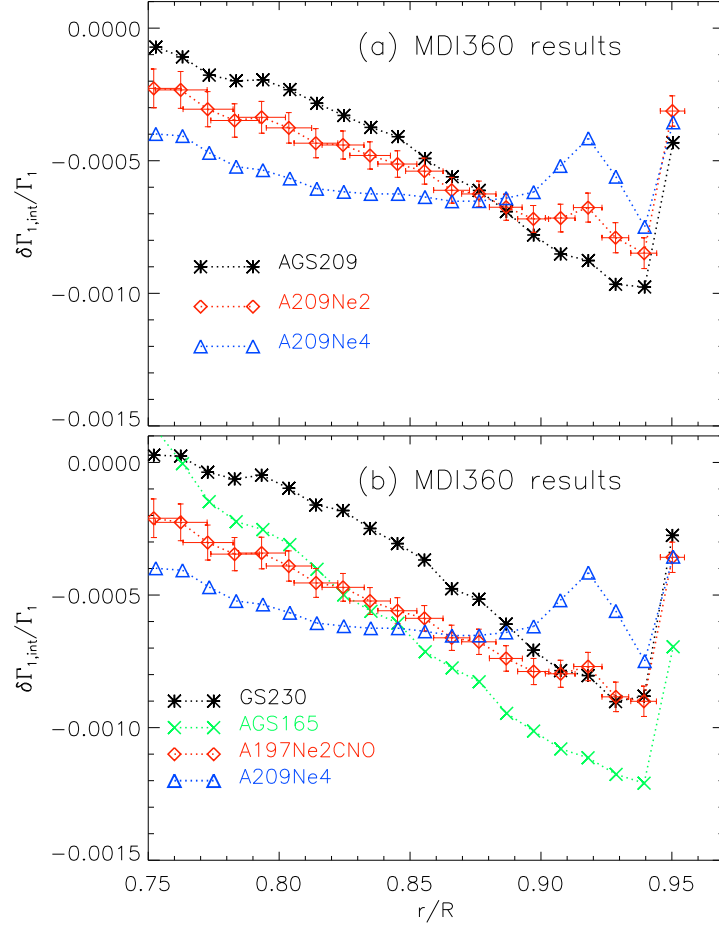


Fig. 6.— The effect of neon enhancement on the $\Gamma_{1,\text{int}}$ differences between the Sun and models. (a) The effect of enhancing neon abundance when Z/X is kept the same. (b) The effect of changing Z/X as the neon abundance is enhanced. The two neon-enhanced models are the ones proposed by Antia & Basu (2005) to get models with the AGS05 abundances to agree with the Sun. A normal AGS05 model and a GS98 model is shown for comparison.